Progress in Natural Science: Materials International 2013;23(3):308–316

Chinese Materials Research Society

Progress in Natural Science: Materials International

www.elsevier.com/locate/pnsmi
www.sciencedirect.com

ORIGINAL RESEARCH

Preparation of ultrahigh surface area porous carbons templated using zeolite 13X for enhanced hydrogen storage

Eric Masika, Robert Mokaya*

School of Chemistry, University of Nottingham, University Park, Nottingham NG7 2RD, UK

Received 23 October 2012; accepted 12 March 2013
Available online 17 May 2013

KEYWORDS

Hydrogen storage;
Zeolite templated carbon;
Zeolite 13X;
High surface area;
Micropores

Abstract In this report, the use of zeolite 13X as a template to generate ultrahigh surface area carbons, via a two-step process combining liquid impregnation and chemical vapour deposition is explored. The first step in the nanocasting process involves impregnation of zeolite 13X with furfuryl alcohol and the second step consists of chemical vapour deposition (CVD) of ethylene at 700 °C. Zeolite-like structural ordering was achieved for zeolite templated carbons (ZTCs) prepared at variable heating ramp rates of 5, 10 or 15 °C/min. The textural properties of ZTCs prepared at all heating ramp rates were comparable with small variations in which the lowest ramp rate (5 °C/min) generated ZTC with highest surface area and pore volume of 3332 m^2/g and 1.66 cm^3/g respectively. The carbon materials achieved a remarkable hydrogen uptake of 7.3 wt% at 20 bar and 77 K which is the highest ever recorded for carbon materials. This report also explores the mechanical stability of the ZTCs via compaction at up to 10*t* (equivalent to 740 MPa) in which the compacted samples showed minimal modification and retained high hydrogen storage capacity.

1. Introduction

In recent years, research on hydrogen storage has been guided mainly by the requirements set forth by the United States Department of Energy (DOE) in 2003 [1]. Revisions to the set targets are on-going based on improved forecasts that come from actual research findings. For example, revisions in 2010 decreased the storage target to 5 wt% (40 g/L) of hydrogen at ambient temperature and pressure <100 bar. One of the most promising methods to store hydrogen is in solid state materials such as

*Corresponding author. Tel.: +44 115 846 6174; fax: +44 115 951 3562.
E-mail address: r.mokaya@nottingham.ac.uk (R. Mokaya).

Peer review under responsibility of Chinese Materials Research Society.

Production and hosting by Elsevier

1002-0071
http://dx.doi.org/10.1016/j.pnsc.2013.04.007

nanostructured porous carbons, because nanoporous carbons have attractive chemical, physical, thermodynamic and transport properties compared to other bulky materials [2].

Nanostructured porous carbons with high surface area and well-ordered pore systems continue to be a very important category of porous materials at nanometre scale for possible application in hydrogen storage [3–8]. There are several encouraging examples of the potential use of porous carbons for hydrogen storage with some classes of carbons showing very high uptake. Yang and co-workers have shown that zeolite templated carbons nanocast using zeolite beta as template can store up to 6.9 wt% hydrogen at 20 bar and 77 K, one of the highest value reported to date [6]. Wang and co-workers reported hydrogen uptake of 7.08 wt% (at 20 bar and 77 K) for a doubly activated carbon [7], while more recently, Sevilla et al. achieved hydrogen uptake capacity of 7.03 wt% under similar conditions for ultrahigh surface area polypyrrole-based activated carbons [8].

Porous carbons are conventionally obtained by carbonisation of precursors of natural or synthetic origin, followed by chemical or physical activation procedures. However, traditional activation procedures lack control over porosity development, leading to materials with broad pore size distribution and disordered structures. On the other hand, hard templating with inorganic frameworks has been the most successful method so far in controlling the porosity of carbons [9–15]. This method involves filling the pores of a solid (as template) with a different material, followed by chemical separation of the resulting material from the template. The success of this method has been demonstrated for the preparation of replica polymers [16,17], metal [18] and semiconductors [19,20], among an ever increasing list of novel porous materials. This report explores the use of suitable templates to prepare carbon materials with controlled architecture and narrow pore size distribution. In particular, the aim is to target templated carbons that possess a significant proportion of micropores below 1.0 nm and preferably in the range 0.6–08 nm as it is known from previous studies that such pores are the most efficient for hydrogen adsorption [8,21–25].

Among the many templates that are currently under intensive research for synthesis of nanostructured carbons, much attention has been paid to zeolites [10,25–28]. Despite extensive investigations into nanocasting techniques, the use of two-step nanocasting has not yet been fully exploited with respect to optimising textural properties for hydrogen storage. This process involves Liquid Impregnation (LI) during which zeolite channels are first filled by a carbon precursor followed by polymerisation of the precursor and partial carbonisation as the first stage. The second stage involves the use of different carbon precursor for Chemical Vapour Deposition (CVD) onto the zeolite/carbon composite obtained in the first step. In this study, the selection of zeolite 13X as a hard template was based on the fact that most studies so far have focused on the use of zeolite Y (FAU-type structure) [9,12,13,29], zeolite beta [6,30] and zeolite EMC-2 (EMT-structure type) [31]. Separately, the effect of compaction on the textural properties of the templated carbons is assessed since such materials are expected to withstand high pressure conditions in some industrial applications. Indeed currently there is no data on the mechanical stability of zeolite-templated carbons under high compaction pressures. Such data is particularly relevant given that other types of materials with potential as hydrogen stores, such as metal organic frameworks (MOFs) or activated carbons (ACs) have poor (MOFs) or moderate (ACs) mechanical stability [31].

2. Experimental section

2.1. Material synthesis

Three carbon samples were prepared using different heating ramp rates. In summary, 0.6 g zeolite 13X was dried in the furnace at 300 °C for 12 h before being impregnated (via incipient wetness method) with furfural alcohol. The resulting FA/zeolite composite was placed on an alumina boat and transferred into a flow through tube furnace and polymerised under argon flow at 80 °C for 24 h followed by further heating at 150 °C for 8 h. In order to allow the carbonisation of polymerised furfural alcohol (polyfurfuryl alcohol), the temperature was ramped at 5 °C/min to 700 °C and held for 3 h under Ar flow. The resulting zeolite/carbon composite was then exposed to ethylene gas (10% in Argon by volume) at 700 °C for 3 h. The gas flow was then switched to Ar flow only and the temperature of the furnace was raised to 900 °C and held for 3 h followed by cooling under Ar to room temperature. The resulting zeolite/carbon composite was treated in 10% HF for 24 h, washed and then refluxed in 36.5% HCl for 6 h. The final carbon was then washed with deionised water and dried at 120 °C for 12 h. Hereinafter the resulting carbon sample is denoted as FA-ZTC1. Two other samples, designated as FA-ZTC2 and FA-ZTC3, were prepared as described above except that a heating ramp rate of 10 and 15 °C/min respectively was used.

To probe the effect of compaction on the textural properties and morphology of the zeolite templated carbons, sample FA-ZTC3 was compacted for 10 min at loads of 5*t* or 10*t* on a 1.3 cm diameter die, equivalent to compaction pressure of 370 MPa and 740 MPa respectively. Briefly, ca. 35 mg of the carbon was loaded into a pressing unit which was then compacted at a load of 5 or 10 t for 10 min. The compacted samples were denoted as C5-FA-ZTC3 and C10-FA-ZTC3 for compaction at a load of 5*t* and 10*t* respectively.

2.2. Materials characterisation

Powder XRD analysis was performed on a Bruker D8 Advance powder diffractometer using CuKα radiation ($\lambda = 1.5406$ Å) and operating at 40 kV and 40 mA, with 0.02° step size and 2 s step time. Thermogravimetric analysis was performed using a TA Instruments SDT Q600 analyser under flowing air conditions. For porosity analysis, each sample was pre-dried in an oven and then degassed overnight at 200 °C under high vacuum. The textural properties were determined by nitrogen sorption at −196 °C using a Micromeritics ASAP 2020 volumetric sorptometer. The surface area was calculated by using the BET method applied to adsorption data in the relative pressure (P/Po) range of 0.06–0.22. The total pore volume was determined from the amount of nitrogen adsorbed at $P/Po = 0.99$. The pore size distribution was determined by a non-local density functional theory (NLDFT) method using nitrogen adsorption isotherms. Transmission Electron Microscopy (TEM) micrographs were recorded on a JEOL 2000-FX with a LaB_6 filament operating at 200 kV. Sample preparation involved ultrasonic dispersion of the solid powders in ethanol followed by several drops being cast onto copper-grid mounted 'holey' carbon films.

2.3. Hydrogen uptake measurements:

Hydrogen uptake capacity of the carbons was measured by gravimetric analysis with an Intelligent Gravimetric Analyser, IGA, (Hiden)

using 99.9999% purity hydrogen additionally purified by a molecular sieve filter. Prior to analysis, the carbon samples were dried in an oven for 24 h at 80 °C overnight and then placed in the analysis chamber and degassed at 200 °C and 10^{-10} bar for 4–6 h. The hydrogen uptake measurements were performed at −196 °C (in a liquid nitrogen bath) over the pressure range 0 to 20 bar. The uptake data was corrected for the buoyancy of the system and samples. The hydrogen uptake was calculated on the basis of a density of 1.5 g/cm^3 for the carbons, and 0.04 g/cm^3 for the adsorbed hydrogen.

3. Results and discussion

3.1. *Structural ordering and thermal stability of templated carbons*

Fig. 1 shows the powder XRD patterns of ZTCs obtained at variable heating ramp rate. For comparison, the XRD patterns for Zeolite 13X and zeolite/carbon composite prior to zeolite etching are included. For all the carbons, the XRD patterns show a sharp peak, similar to that present in the zeolite 13X, at $2\theta = 6.3^\circ$ corresponding to *d*-spacing of ca. 1.4 nm which is comparable to that of zeolite 13X (*d*-spacing = 1.4 nm). This suggests that the resulting ZTCs exhibit structural pore ordering similar to that of zeolite 13X [26,32,33]. In addition a very broad and weak peak is observed at $2\theta = 43^\circ$ which is attributed to (101) diffraction from graphitic/turbostratic carbon [34]. The weak peak observed at $2\theta = 43^\circ$ could be attributed to the presence a thin layer of turbostratic carbon deposited on the outer surface of the zeolite particles [26,29,35]. However, worth noting is the near complete absence of a peak at $2\theta = 26^\circ$, usually ascribed to the (002) diffraction of graphitic carbon. The XRD patterns of zeolite 13X and the zeolite/carbon composite (Fig. 1) are characterised by the appearance of many sharp peaks due to the framework topology of zeolite 13X. The presence of these peaks is evidence that the zeolite framework is not destroyed upon carbonisation and heat treatment at temperatures of up to 900 °C. However, it is worth noting that the intensity of zeolite structural peaks is significantly reduced as expected in the composite due to the filling of zeolite pores, which causes reduction in phase contrast scattering.

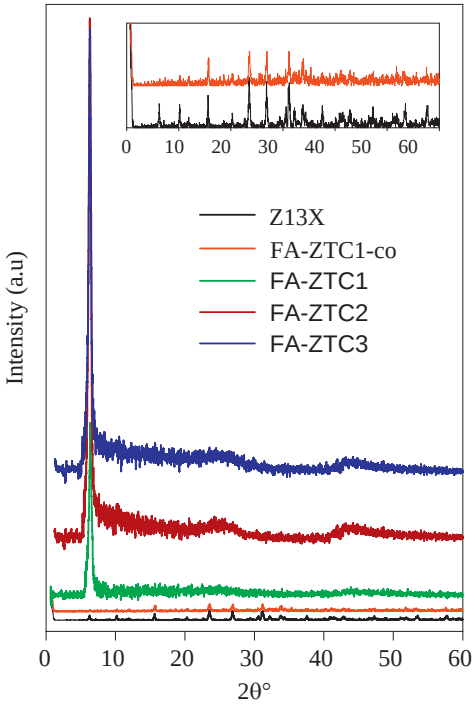

Fig. 1 Powder XRD patterns of zeolite templated carbons (FA-ZTC1, FA-ZTC2 and FA-ZTC3) prepared at variable heating ramp rate (5, 10 and 15 °C/min respectively). Patterns for the zeolite/carbon composite (FA-ZTC1-co) and zeolite 13X (Z13X) are also shown.

It is reasonable to infer that the FA-ZTCn samples are essentially amorphous (i. e. non-graphitic) with respect to crystallographic ordering. This is evident from the absence of the peak at $2\theta = 26^\circ$, as well as the presence of a weak and broad peak at $2\theta = 43^\circ$. This is because at 700 °C (which is the CVD temperature used for synthesis of FA-ZTCn samples) the carbonisation process is relatively slow and the ethylene in the second step is able to permeate into the zeolite/polyfurfuryl alcohol composite and enter into any unfilled zeolite pores. The preferential internal deposition of carbon into zeolite particles has been reported by Alam and Mokaya to enhance the replication of zeolite-like pore channel regularity in the resulting carbon materials [12]. Moreover, given the narrow nanochannels of zeolite 13X, it is impossible to form stacking structures within the pores and therefore the expectation is that the resultant carbons will comprise of a single graphene sheet without any stacking and are thus are non-graphitic [36]. Overall, the XRD patterns indicate that the heating ramp rate had negligible effect on the structural ordering of the resultant carbons but exerts a small effect on the nature of the carbon; the broad peak at $2\theta = 43^\circ$ is slightly more prominent for samples prepared at higher heating ramp rates (FA-ZTC2 and FA-ZTC3), while for FA-ZTC1 the peak is virtually absent.

The thermal stability of the FA-ZTC samples was probed by thermogravimetric analysis (TGA). Fig. 2 shows the TGA curves of the zeolite template (Z13X), a representative zeolite/carbon composite (FA-ZTC1-Co) and carbon (FA-ZTC1). The TGA curve of the zeolite 13X template shows a weight loss event of ca. 10% in the temperature range 180 °C to 350 °C which is

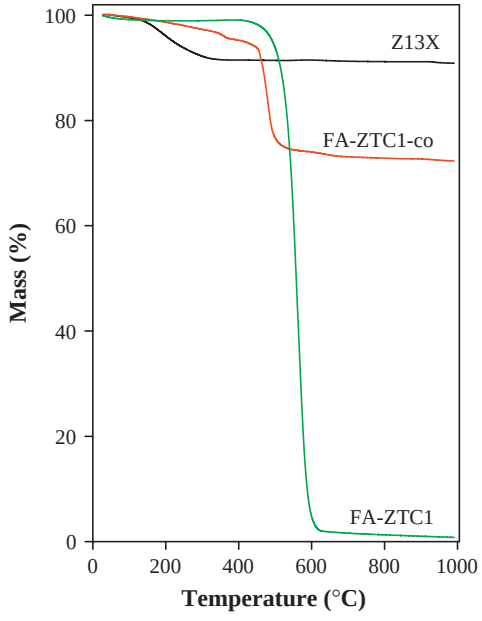

Fig. 2 TGA curves for zeolite 13X (Z13X), zeolite/carbon composite (FA-ZTC1-co) and zeolite template carbon (FA-ZTC1).

attributable to removal of water. As expected after this early weight loss, the zeolite is stable up to 1000 °C. The TGA curve for the zeolite/carbon composite (FA-ZTC1-Co) exhibits a single weight loss between 400 °C and 560 °C due to the combustion of the carbon component. The percentage of carbon in the zeolite/carbon composite was determined to be ca. 28%, which is an amount large enough to allow the replication of zeolite-like ordering [37]. The TGA of the representative template free sample (FA-ZTC1) shows that the carbons exhibit a residual weight of $<2\%$ at 620 °C thus confirming that the ZTCs are virtually zeolite-free. In addition, it is clear that the carbon samples are a one phase materials given the sharp weight loss that occurs in the temperature range 450–610 °C.

3.2. *Porosity of zeolite templated carbons*

Nitrogen sorption isotherms and corresponding pore size distribution curves of the zeolite templated carbons prepared at various heating ramp rates are shown in Fig. 3. For comparison, the data for the zeolite 13X template is also presented. The nitrogen sorption isotherms of all the carbons are mainly type I, with a high nitrogen uptake in the low relative pressure domain ($P/Po<0.01$). The isotherms reveal the super-microporous character of the carbon materials (1.0 nm $<$ pore diameter $<$ 2.0 nm). The isotherms of all the FA-ZTCx samples exhibit hysteresis over a wide range of relative pressure ($P/Po=0.01$ to 0.99) which has previously been reported for some zeolite templated carbons [12,27,38]. The isotherms are consistent with data previously reported for zeolite template carbons that exhibit significant levels of zeolite-like ordering. The pore size distribution curves for the templated carbons, obtained using nonlocal density function theory (NLDFT) are presented in Fig. 3B [39]. The FA-ZTCs exhibit unimodal pore size distribution centred at 1.2 nm; the pore size maxima values are summarised in Table 1. The obtained pore size of 1.2 nm is consistent with previous studies that have shown that zeolite templated carbons with higher levels of zeolite-like ordering do not possess a significant proportion of pores larger than 1.5 nm [6,15,34]. Fig. 3B also indicates that sample FA-ZTC3, which was prepared at the highest heating ramp rate, possess some pores of size ca. 1.9 nm. These larger micropores may be generated due to quicker pore filling or carbonisation process in the zeolite template pores, which may result in a slightly less efficient replication process. We have previously shown that efficient replication of zeolite ordering in the carbons depends on a gradual build-up of carbon precursor within the zeolite template pores. [6,12,15,37]

Table 1 gives the textural parameters and hydrogen uptake of the FA-ZTCn carbons, along with data for the zeolite 13X template. All the carbons possess high surface area and large pore volume of 3106–3332 m^2/g and 1.50–1.66 cm^3/g respectively, which is amongst the highest reported for zeolite templated carbons. The high surface area of FA-ZTCs may be attributed to the presence of single nanographene sheet with surface available as described by Nishihara and co-workers [36]. Moreover, the graphene sheet at nanometre scale consists of a large number of edges, which contribute to an increase in specific surface area. Sample FA-ZTC1 has slightly higher textural properties, which is consistent with the XRD patterns that indicate that the sample has the lowest level of turbostratic/graphitic character. It is also likely that for samples FA-ZTC2 and FA-ZTC3, their slightly more turbostratic/graphitic nature leads to lower surface area. Thus a slow ramping rate favours materials with slightly higher surface area and pore volume. Noteworthy is the proportion of micropore surface area and pore volume which is significantly high; typically up to 88% of the total surface area, while the micropore volume contributes up to 75% of the total pore volume. This agrees with the fact that a high level of zeolite-type pore ordering, as indicated

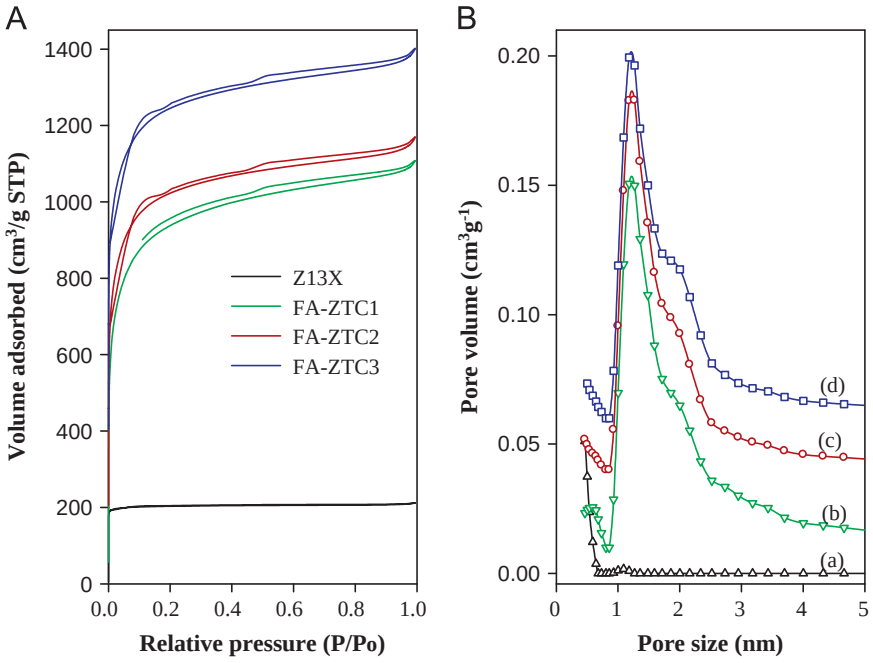

Fig. 3 Nitrogen sorption isotherms (A) and pore size distribution curves (B) for (a) zeolite 13X, (b) FA-ZTC1, (c) FA-ZTC2 and (d) FA-ZTC3. For clarity, sorption isotherms of FA-ZTC2 and FA-ZTC3 are offset (y-axis) by 200 cm^3/g and 400 cm^3/g respectively, and the PSD curves (b), (c) and (d) are offset (y-axis) by 0.01, 0.04 and 0.06 cm^3/g respectively.

Table 1 Textural properties and hydrogen uptake of FA-ZTCn templated carbons. Textural data for zeolite 13X is included for comparison.

Sample	Surface area (m^2/g)[a]	Pore volume (cm^3/g)[b]	Pore size (nm)[c]	H_2 uptake	
				(wt%)[d]	density (ρ)[e]
Z13X	658 (646)	0.33 (0.31)	1.0	–	–
FA-ZTC1	3332 (2837)	1.66 (1.18)	1.2	7.3	11.0
FA-ZTC2	3106 (2728)	1.50 (1.13)	1.2	6.6	10.6
FA-ZTC3	3169 (2760)	1.55 (1.15)	1.2	6.2	9.8

[a]values in the parenthesis are micropore surface area.
[b]values in the parenthesis are micropore volume.
[c]maxima of the PSD obtained using NLDFT analysis.
[d]hydrogen uptake capacity at 77 K and 20 bar.
[e]hydrogen uptake density (ρ) in μmol.H_2 m^{-2}.

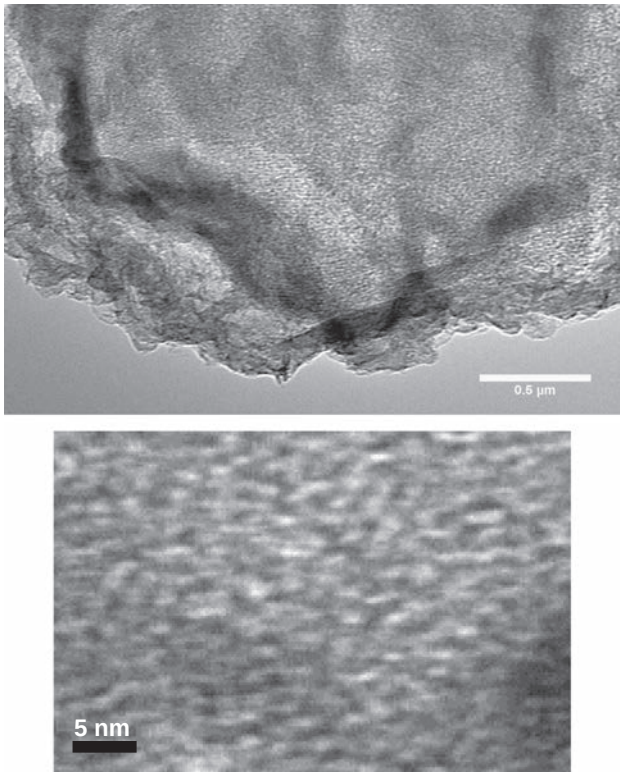

Fig. 4 TEM images of zeolite templated carbon (sample FA-ZTC2).

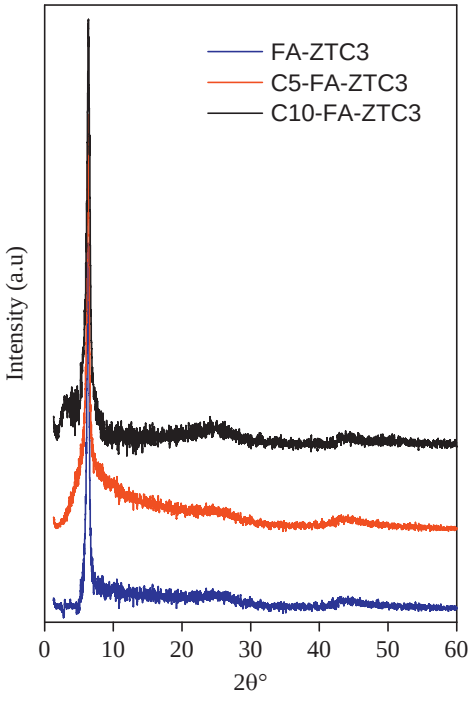

Fig. 5 Powder XRD patterns of zeolite templated carbon (FA-ZTC3) before and after compaction at 5*t* (C5-FA-ZTC3) and 10*t* (C10-FA-ZTC3).

by XRD patterns (Fig. 1), favours high surface area and large pore volume with sizable proportion of microporosity.

3.3. *Nanoscale ordering of zeolite templated carbons*

A representative transmission electron micrograph recorded for sample FA-ZTC2 is presented in Fig. 4. The TEM micrographs clearly reveal well-aligned micropore channels, which is consistent with XRD patterns in Fig. 1. The formation of well-ordered microporous carbon further confirms that the amount of carbon infiltrated into the zeolite channels via the two-step synthesis method was sufficient. Noteworthy is the absence of any significant outer layer covering the particles, which rules out the possibility of graphitisation arising from carbon deposited on the external surface of the zeolite particle.

3.4. *Assessment of mechanical stability of FA-ZTCs*

The mechanical stability of the carbon (FA-ZTC3) prepared at highest heating ramp rate was investigated via compaction at 5*t* (370 MPa) and 10*t* (740 MPa), i.e., 5*t* and 10*t* load on a 1.3 cm diameter die. Fig. 5 shows powder XRD patterns of FA-ZTC3 before and after compaction. The powder XRD patterns in Fig. 5 do not change after compaction; the sharp peak, similar to that present in the zeolite 13X, at $2\theta = 6.3^\circ$ with d-spacing of ca. 1.4 nm is retained after compaction. This indicates that the carbon framework of the zeolite templated carbon can withstand mechanical pressure as high as 740 MPa for 10 min. The structural

ordering remains the same after being exposed to such high compaction pressure.

Nitrogen sorption isotherms and corresponding pore size distribution (PSD) curves for FA-ZTC3 before and after compaction are shown in Fig. 6. Although the shape of the isotherms does not change after compaction, retaining a type I isotherm typical of microporous materials [40], the compacted samples have slightly lower adsorption. The PSD curves in Fig. 6 clearly show that the pore size remains largely unchanged after compaction. Textural properties summarised in Table 2 provide further evidence of negligible modifications in the porosity of the zeolite templated carbons after compaction at a load of 5*t*, and minor reduction after compaction at a load of 10*t*. The surface area of C10-FA-ZTC3 (2782 m^2/g) and pore volume (1.27 cm^3/g) confirms that, at a compaction pressure of 740 MPa (load of 10*t*), the sample is only slightly modified. The small reduction in porosity suggests that rather than a collapse of the ZTC framework, it is more likely that blocking of some pores occurs during the compaction process, which in turn reduces the exposed surface area as well as the pore volume. Also, worth noting is the constant proportion of microporosity in FA-ZTC3 and its compacted derivatives (C5-FA-ZTC3 and C10-FA-ZTC3) which remains unchanged at 87% before and after compaction. Likewise, the compacted zeolite template carbons have significant proportion of micropore volume of up to 74% of the total pore volume.

3.5. *Hydrogen uptake*

The hydrogen uptake isotherms obtained by gravimetric analysis at 77 K and pressures up to 20 bar are shown in Fig. 7. The corresponding hydrogen uptake and hydrogen uptake density at 20bar and 77 K are summarised in Table 1. The isotherms show no hysteresis, which indicates that the hydrogen uptake is totally reversible. In addition, it is clear that the isotherms do not attain uptake saturation at 20 bar which implies that higher capacity for hydrogen storage is possible above 20 bar. Sample FA-ZTC1, which has the highest surface area and micropore surface area of

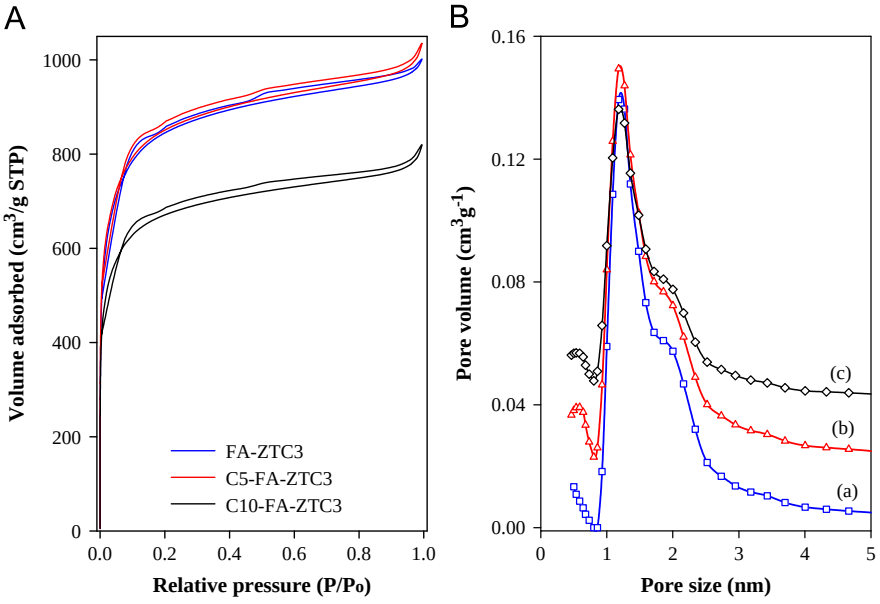

Fig. 6 (A) Nitrogen sorption isotherms and (B) corresponding pore size distribution curves of zeolite templated carbon (FA-ZTC3) before and after compaction at 5*t* (C5-FA-ZTC3) and 10*t* (C10-FA-ZTC3).

Table 2 Textural properties and hydrogen uptake of zeolite template carbon, FA-ZTC3, before and after compaction at a load of 5*t* (C5-FA-ZTC3) or 10*t* (C10-FA-ZTC3).

Sample	Surface area (m^2/g)[a]	Pore volume (cm^3/g)[b]	Pore size (nm)[c]	H_2 uptake	
				(wt%)[d]	density (ρ)[e]
FA-ZTC3	3169 (2760)	1.55 (1.15)	1.2	6.2	9.8
C5-FA-ZTC3	3192 (2769)	1.60 (1.15)	0.6/1.2	6.3	9.9
C10-FA-ZTC3	2782 (2430)	1.27 (0.91)	0.6/1.2	5.9	10.6

[a]values in the parenthesis are micropore surface area.
[b]values in the parenthesis are micropore volume.
[c]maxima of the PSD obtained using NLDFT analysis.
[d]hydrogen uptake capacity at 77 K and 20 bar.
[e]hydrogen uptake density (ρ) in μmol.H_2 m^{-2}.

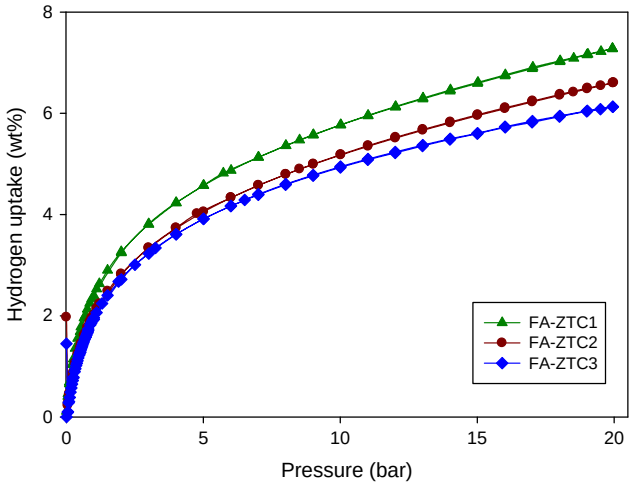

Fig. 7 Hydrogen uptake isotherms of zeolite templated carbons at 77 K.

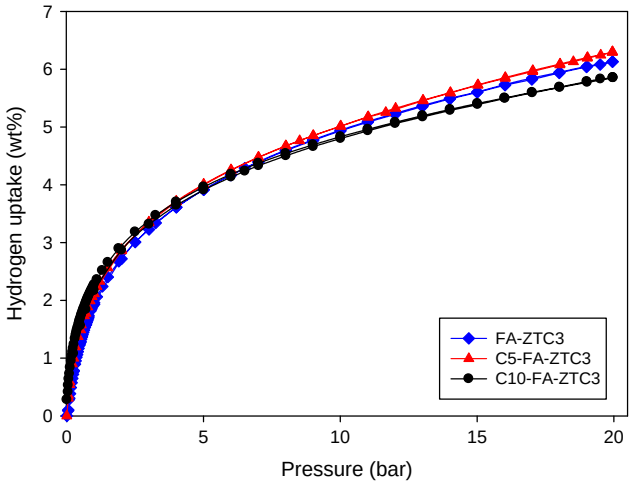

Fig. 8 Hydrogen uptake isotherms at 77 K of zeolite templated carbon (FA-ZTC3) before and after compaction at 5*t* (C5-FA-ZTC3) and 10*t* (C10-FA-ZTC3).

3332 and 2837 m^2/g respectively, exhibits the highest hydrogen uptake capacity of 7.3 wt% at 20 bar and 77 K. The hydrogen uptake then slightly reduces for samples FA-ZTC2 (6.6 wt%) and FA-ZTC3 (6.2 wt%), due to their slightly lower surface area. The hydrogen uptake density of between 10 and 11 μmol H_2/m^{-2} is in line with what has previously been reported for similar ZTC materials [6,12,15,37]. Overall, the present samples exhibit hydrogen uptake that is at the very top of the range known for carbon materials. Indeed, it is worth noting that the 7.3 wt% uptake of sample FA-ZTC1 is the highest ever recorded for any carbon material [21,41–49]. This result surpasses the 6.9 wt% previously reported for a zeolite EMC-2 templated carbon [6], 7.03 wt% for a Polypyrrole-derived activated carbon [8] and 7.08 wt% for a doubly activated carbon [7].

The high uptake of the present samples is attributed to well-controlled pore size centred at 1.2 nm as well as the high surface area. Indeed, sample FA-ZTC1 not only exhibits the highest surface area put also the narrowest pore size distribution with fewer larger pores (Fig. 3) compared to the other two samples. It is noteworthy that sample FA-ZTC1 has an excess hydrogen uptake of 6.2 wt% and a projected maximum total hydrogen adsorption capacity of up to 9.22 wt% (equivalent to hydrogen uptake density of 13.8 μmol H_2/m^2); the maximum hydrogen uptake is obtained via extrapolation by fitting the adsorption data at 77 K with the Langmuir model [50]. The unprecedented high hydrogen storage exhibited by sample FA-ZTC1 provides further evidence that zeolite templated carbons remain one of the key materials for use in gas storage. Overall, the optimal pore size and pore size distribution of ZTCs along with high surface area offer an excellent base for enhanced hydrogen storage.

The hydrogen uptake capacity for FA-ZTC3 and its compacted derivatives is shown in Fig. 8. Table 2 gives the hydrogen uptake at 20 bar. Interestingly, the hydrogen uptake capacity after compaction at a load of 5*t* (370 MPa) was virtually unchanged, which is consistent with the non-changing textural properties. After compaction at a load of 10*t* (740 MPa), there was a very slight decrease in hydrogen uptake, which again is consistent with the small decrease in surface area. Overall, the small variations in the hydrogen uptake before and after compaction may be attributed to the increased packing density of carbons after compaction at higher pressure without much change in porosity [51,52]. The changes in hydrogen uptake capacities may be attributed to

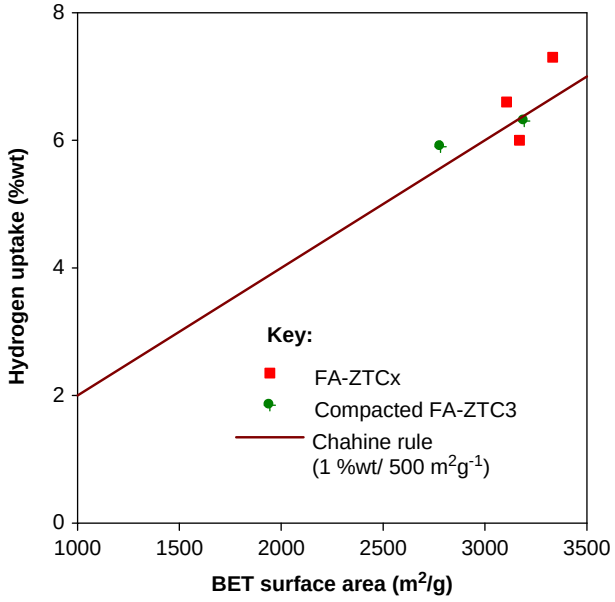

Fig. 9 Correlation between surface area and hydrogen uptake capacity for FA-ZTC samples.

modification of the specific interparticle pore volume upon compaction [53]. This results are remarkable given that other high surface area materials such as MOFs (i.e., MOF-5) are irreversibly destroyed after compaction at 180 MPa while ZIFs are stable only up to 340 MPa [37]. Activated carbons with moderate surface area have been shown to be stable up to a compaction pressure of 420 MPa [37].

Generally, the FA-ZTCs recorded hydrogen uptake capacity that tends to outperform or is in line with the Chahine rule as illustrated in Fig. 9 [54]. The Chahine rule is a widely accepted relationship which states that in general there is 1 wt% hydrogen adsorption for every 500 m^2/g of surface area. This is equivalent to a hydrogen density of 10 μmol H_2/m^2. Therefore, the FA-ZTCn carbons generally showed superior hydrogen uptake as compared to the average for carbonaceous materials. According to Fig. 9, the hydrogen uptake capacity is closely related to the surface area of

the carbons which is in agreement with most previously reported data [34,55]. Overall, the higher hydrogen uptake is attributed to the presence of optimal pore size range and that of an enclosed surface area with high proportion of micropores. FA-ZTCs have PSD with maximum centred at 1.2 nm. This agrees with Fisher and co-workers who concluded that pores larger than 1.5 nm make little contribution to hydrogen uptake at 77 K and pressure of up to 60 bar [55].

4. Summary

A nanocasting technique via a two-step synthesis process has been employed to generate a suite of porous carbons with zeolite-like structural ordering. It was found that the heating ramp rate used in getting to the carbonisation temperature of 700 °C has only small effects on the textural properties while compaction (up to 740 MPa) of the carbons resulted in slight modification of porosity. All the templated carbons, irrespective of whether compacted or not exhibit high surface area and large pore volume of up to 3332 m^2/g and 1.66 cm^3/g respectively. The porosity in the templated carbons consisted of micropores with a unimodal pore size distribution centred at 1.2 nm. The templated carbons have a total hydrogen uptake capacity of up to 7.3 wt% at 20 bar and 77 K, excess hydrogen uptake of 6.2 wt% and projected maximum uptake capacity of 9.22 wt% (equivalent to hydrogen uptake density of 13.8 μmol H_2/m^2), which are the highest values ever reported for a carbon material. This study highlights a promising route for synthesis and post synthesis modification of carbon materials with tuneable porosity. The findings add new insights that are valuable for the development of carbonaceous materials with enhanced hydrogen storage capacity.

Acknowledgements

This research was funded by the University of Nottingham, and the EPSRC.

References

[1] Fuel cell technologies program multi-year research, development and demonstration plan, The DOE Hydrogen and Fuel Cells Program, ⟨http://www1.eere.energy.gov/hydrogenandfuelcells/mypp/⟩.
[2] A.M. Seayad, D.M. Antonelli, Advanced Materials 16 (2004) 765–777.
[3] A.W.C. van den Berg, C.O. Arean, Chemical Communications (2008) 668–681.
[4] (a) R. Ströbel, L. Jörissen, T. Schliermann, V. Trapp, W. Schütz, K. Bohmhammel, G. Wolf, J. Garche, Journal of Power Sources 84 (1999) 221–224;
(b) K.M. Thomas, Catalysis Today 120 (2007) 389–398.
[5] (a) M. Sevilla, A.B. Fuertes, R. Mokaya, Energy and Environmental Science 4 (2011) 1400–1410;
(b) M. Sevilla, R. Foulston, R. Mokaya, Energy and Environmental Science 3 (2010) 223;
(c) M. Sevilla, A.B. Fuertes, R. Mokaya, International Journal of Hydrogen Energy 36 (2011) 15658;
(d) A. Almasoudi, R. Mokaya, Journal of Materials Chemistry 22 (2012) 146;
(e) Y. Xia, R. Mokaya, Chemical Vapor Deposition 16 (2010) 322.
[6] Z. Yang, Y. Xia, R. Mokaya, Journal of the American Chemical Society 129 (2007) 1673–1679.
[7] H. Wang, Q. Gao, J. Hu, Journal of the American Chemical Society 131 (2009) 7016–7022.
[8] M. Sevilla, R. Mokaya, A.B. Fuertes, Energy and Environmental Science 4 (2011) 2930–2936.
[9] T. Kyotani, Bulletin of the Chemical Society of Japan 79 (2006) 1322–1337.
[10] Y. Xia, Z. Yang, R. Mokaya, Nanoscale 2 (2010) 639–659.
[11] A.A. Zakhidov, R.H. Baughman, Z. Iqbal, C. Cui, I. Khayrullin, S.O. Dantas, J. Marti, V.G. Ralchenko, Science 282 (1998) 897–901.
[12] N. Alam, R. Mokaya, Energy and Environmental Science 3 (2010) 1773–1781.
[13] J. Lee, J. Kim, T. Hyeon, Advanced Materials 18 (2006) 2073–2094.
[14] R. Ryoo, S.H. Joo, M. Kruk, M. Jaroniec, Advanced Materials 13 (2001) 677–681.
[15] Y. Xia, G.S. Walker, D.M. Grant, R. Mokaya, Journal of the American Chemical Society 131 (2009) 16493–16499.
[16] R.V. Parthasarathy, C.R. Martin, Nature 369 (1994) 298–301.
[17] S.A. Johnson, P.J. Ollivier, T.E. Mallouk, Science 283 (1999) 963–965.
[18] C.R. Martin, Advanced Materials 3 (1991) 457–459.
[19] C. West, R. Mokaya, Chemistry of Materials 21 (2009) 4080–4086.
[20] J.D. Klein, R.D. Herrick, D. Palmer, M.J. Sailor, C.J. Brumlik, C.R. Martin, Chemistry of Materials 5 (1993) 902–904.
[21] N. Texier-Mandoki, J. Dentzer, T. Piquero, S.-E. Saadallah, P. David, C. Vix-Guterl, Carbon 24 (2004) 2744–2747.
[22] I. Cabria, M.J. López, J.A. Alonso, Carbon 45 (2007) 2649–2658.
[23] G. Yushin, R. Dash, J. Jagiello, J.E. Fischer, Y. Gogotsi, Advanced Functional Materials 16 (2006) 2288–2293.
[24] Y. Gogotsi, R.K. Dash, G. Yushin, T. Yildirim, G. Laudisio, J.E. Fischer, Journal of the American Chemical Society 127 (2005) 16006–16007.
[25] M. Sevilla, N. Alam, R. Mokaya, Journal of Physical Chemistry C 114 (2011) 11314–11319.
[26] T. Kyotani, Z. Ma, A. Tomita, Carbon 41 (2003) 1451–1459.
[27] (a) T. Kyotani, T. Nagai, S. Inoue, A. Tomita, Chemistry of Materials 9 (1997) 609–615;
(b) Z. Ma, T. Kyotani, A. Tomita, Carbon 40 (2002) 2367–2374.
[28] P. Enzel, T. Bein, Chemistry of Materials 4 (1992) 819–824.
[29] A. Pacula, R. Mokaya, Journal of Physical Chemistry C 112 (2008) 2764–2769.
[30] C. Ducrot-Boisgontier, J. Parmentier, J. Patarin, Microporous and Mesoporous Materials 126 (2009) 101–106.
[31] (a) K.W. Chapman, G.J. Halder, P.J. Chupas, Journal of the American Chemical Society 131 (2009) 17546–17547;
(b) J. Alcaniz-Monge, G. Trautwein, M. Perez-Cadenas, M.C. Roman-Martinez, Microporous and Mesoporous Materials 126 (2009) 291–301.
[32] F.O.M. Gaslain, J. Parmentier, V.P. Valtchev, J. Patarin, Chemical Communications (2006) 991–993.
[33] Z. Yang, Y. Xia, R. Mokaya, Microporous and Mesoporous Materials 86 (2005) 69–80.
[34] Z.X. Yang, Y.D. Xia, X.Z. Sun, R. Mokaya, Journal of Physical Chemistry B 110 (2006) 18424–18431.
[35] Z. Ma, T. Kyotani, A. Tomita, Chemical Communications (2000) 2365–2366.
[36] H. Nishihara, Q.-H. Yang, P.-X. Hou, M. Unno, S. Yamauchi, R. Saito, J.I. Paredes, A. Martínez-Alonso, J.M.D. Tascón, Y. Sato, M. Terauchi, T. Kyotani, Carbon 47 (2009) 1220–1230.
[37] (a) Y. Xia, R. Mokaya, D.M. Grant, G.S. Walker, Carbon 49 (2011) 844;
(b) N. Alam, R. Mokaya, Microporous and Mesoporous Materials 142 (2011) 716;
(c) N. Alam, R. Mokaya, Microporous and Mesoporous Materials 144 (2011) 140.
[38] (a) S.A. Johnson, E.S. Brigham, P.J. Ollivier, T.E. Mallouk, Chemistry of Materials 9 (1997) 2448–2458;
(b) F. Su, X.S. Zhao, L. Lv, Z. Zhou, Carbon 42 (2004) 2821–2831.
[39] C. Guan, K. Wang, C. Yang, X.S. Zhao, Microporous and Mesoporous Materials 118 (2009) 503–507.
[40] K.S.W. Sing, D.H. Everett, R.A.W. Haul, L. Moscou, R.A. Pierotti, J. Rouquerol, T. Siemieniewska, Pure Applied Chemistry 57 (1985) 603–619.

[41] M. Armandi, B. Bonelli, C.O. Areán, E. Garrone, Microporous and Mesoporous Materials 112 (2008) 411–418.
[42] P. Chen, X. Wu, J. Lin, K.L. Tan, Science 285 (1999) 91–93.
[43] M. Hirscher, B. Panella, Journal of Alloys and Compounds 404–406 (2005) 399–401.
[44] C. Liu, Y.Y. Fan, M. Liu, H.T. Cong, H.M. Cheng, M.S. Dresselhaus, Science 286 (1999) 1127–1129.
[45] M. Rzepka, P. Lamp, M.A. de la Casa-Lillo, Journal of Physical Chemistry B 102 (1998) 10894–10898.
[46] L. Schlapbach, A. Zuttel, Nature 414 (2001) 353–358.
[47] E. Terrés, B. Panella, T. Hayashi, Y.A. Kim, M. Endo, J.M. Dominguez, M. Hirscher, H. Terrones, M. Terrones, Chemical Physics Letters 403 (2005) 363–366.
[48] Y. Xia, R. Mokaya, Journal of Physical Chemistry C 111 (2007) 10035–10039.
[49] W.C. Xu, K. Takahashi, Y. Matsuo, Y. Hattori, M. Kumagai, S. Ishiyama, K. Kaneko, S. Iijima, International Journal of Hydrogen Energy 32 (2007) 2504–2512.
[50] G. Srinivas, Y. Zhu, R. Piner, N. Skipper, M. Ellerby, R. Ruoff, Carbon 48 (2010) 630–635.
[51] J. Juan-Juan, J.P. Marco-Lozar, F. Suárez-García, D. Cazorla-Amorós, A. Linares-Solano, Carbon 48 (2010) 2906–2909.
[52] J. Alcañiz-Monge, G. Trautwein, M. Pérez-Cadenas, M.C. Román-Martínez, Microporous and Mesoporous Materials (2009) 291–301.
[53] P.X. Hou, H. Orikasa, H. Itoi, H. Nishihara, T. Kyotani, Carbon 45 (2007) 2011–2016.
[54] (a) P. Bénard, R. Chahine, Scr. Mater. 56 (2007) 803–808;
(b) E. Poirier, R. Chahine, T.K. Bose, International Journal of Hydrogen Energy 26 (2001) 831–835.
[55] Y. Gogotsi, C. Portet, S. Osswald, J.M. Simmons, T. Yildirim, G. Laudisio, J.E. Fischer, International Journal of Hydrogen Energy 34 (2009) 6314–6319.